Molecular Crystals and Liquid Crystals

Publication details, including instructions for authors and subscription information:
http://www.tandfonline.com/loi/gmcl20

Mesoscale Three Dimensional Lattices Formed in Polymer Dispersed Liquid Crystals: A Diamond-Like Face Centered Cubic

Michael Escuti [a] & Gregory Crawford [a]

[a] Division of Engineering, Brown University, Providence, RI, USA

Version of record first published: 18 Oct 2010

To cite this article: Michael Escuti & Gregory Crawford (2004): Mesoscale Three Dimensional Lattices Formed in Polymer Dispersed Liquid Crystals: A Diamond-Like Face Centered Cubic, Molecular Crystals and Liquid Crystals, 421:1, 23-36

To link to this article: http://dx.doi.org/10.1080/15421400490501158

Mol. Cryst. Liq. Cryst., Vol. 421, pp. 23–36, 2004

ISSN: 1542-1406 print/1563-5287 online
DOI: 10.1080/15421400490501158

Taylor & Francis
Taylor & Francis Group

MESOSCALE THREE DIMENSIONAL LATTICES FORMED IN POLYMER DISPERSED LIQUID CRYSTALS: A DIAMOND-LIKE FACE CENTERED CUBIC

Michael J. Escuti and Gregory P. Crawford
Brown University, Division of Engineering, Box D,
Providence, RI 02912 USA

Mesoscale three-dimensional lattices are formed in polymer-dispersed liquid crystals using one-step holographic fabrication. Nematic liquid crystal domains are patterned within a rigid polymer binder through an irradiance-driven diffusion and phase-separation process, forming a low index-contrast photonic crystals whose dielectric profile mimics the irradiance profile applied during formation. Electric fields are used to align the liquid crystal domains, allowing electrical control of the coherent scattering from these lattices. Here we present a diamond-like face centered-cubic-lattice (fcc), highlighting the several advantages over the simple fcc counterpart, including easier processing, operation in the near infrared, and deeper stopbands.

Keywords: diamond-like face-centered-cubic; holography; H-PDLC; mesoscale lattices; photonic crystals

1. INTRODUCTION

While ongoing development of polymer dispersed liquid crystals (PDLCs) continues [1], a renewed interest in the development of a stratified version of PDLCs for several emerging applications has appeared. This descendent involves a holographic photo-polymerization exposure process that creates a stratified composite material of alternating liquid crystal-rich and polymer-rich planes on the submicrometer scale. These materials are known

The authors wish to acknowledge the National Science Foundation (ECS 0322878) and the NASA Graduate Student Researchers Program.

Address correspondence to Gregory P. Crawford, STO 0.26: Polymer Technology, Department of Chemical Engineering and Chemistry, Eindhoven University of Technology, P.O. Box 513, 5600 MB, Eindoven, The Netherlands. E-mail: g.crawford@tue.nl

as holographic polymer dispersed liquid crystals (H-PDLCs) [2]. Essentially switchable holographic materials, simple and complex diffraction gratings of all varieties can be recorded and replayed using most of the techniques in holography [3,4]. H-PDLCs offer a broad scope of functionality and attractive features based on the principle of an electrically controllable index modulation, including sub-millisecond response times, extraordinary wavelength selectivity, and the flexibility to tailor the diffraction/reflection properties from UV to near-infrared wavelengths. The combination of diffraction/reflection, possible tunability, and switchability in a single film (typically 5–25 μm thick) has the potential to enable new applications based on Bragg phenomena, and potentially add functionality to existing Bragg devices.

A variety of new devices using H-PDLC have been proposed, including low-power color reflective displays [5–7], telecommunication switches [8,9], polarization selective projection components [10], switchable lenses [11], photonic crystals [12–17], mirrorless lasing [18], laser wavelength dosimetry badges [19], optical strain gauges [20], image capture systems [21], beam steering [22], optical data storage [23,24], remote sensing [25], active U-turn switches [26], and application specific lenses [27]. There have been many basic studies on optical behavior [28–31], electro-optic switching [32], liquid crystal ordering [33], and polymer morphologies [34–36]. Within the last few years, a number of new configurations have been reported, such as those based on polymer networks [37–39], polarization independent switching configurations [40], smectic-A phases [41], two-photon induced polymerization renditions [42], tunable reflection modes [43], specialized holographic methods [44–46], diffuse reflection modes [47], azo-dye doped PDLCs [48,49], thermal switching modes [50], and total internal reflection configurations [51]. Figure 1(a) illustrates how a red, green, blue H-PDLC stack (electrically switchable color filter stack) can be used in digital imaging using a single CCD [21] and Figure 1(b) illustrates the operation of a four-channel add-drop filter for telecommunication applications [22]. These are only two examples of the potential application of electrically switchable filters/gratings based on H-PDLC technology.

As with conventional PDLCs [1], these materials are basically composed of a homogeneous mixture of reactive monomer(s), photoinitiator, and nematic liquid crystal sandwiched between two conducting glass plates. A holographic exposure process is subsequently applied, where two (or more) beams of coherent laser light interfere and create spatially structured light. An example is illustrated in Figure 2(a) for a one-dimensional reflection grating formed by two interfering coherent beams, where the pitch, $\Lambda = \lambda_f / 2 n_0 \sin\Theta$, is expressed in terms of half the angle between exposing beams (Θ), the average index of the material (n_0), and the formation wavelength (λ_f) used during exposure. The resulting H-PDLC film

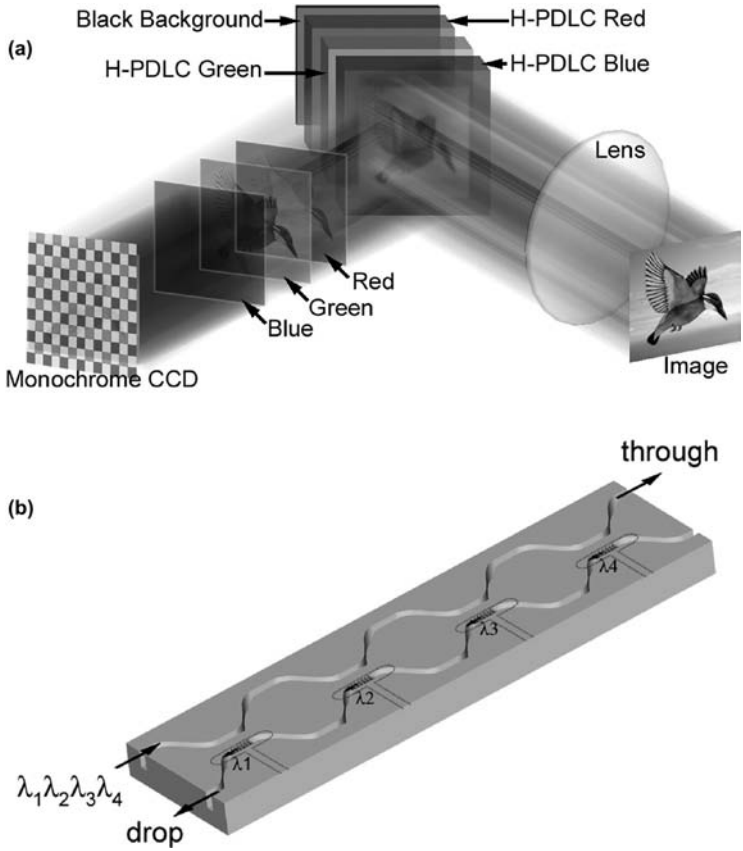

FIGURE 1 Example applications of H-PDLCs: (a) a three panel stack that temporally directs a red, green, and blue image to a monochrome CCD, and (b) a four-channel add-drop switchable waveguide device based on evanescent coupling.

captures this irradiance profile indefinitely, and will reflect according to Bragg's Law (Fig. 2(b)), where the reflective wavelength is given by the expression, $\lambda_R = 2n_0\Lambda\sin\theta$, with θ being the angle between the plane of the substrate and the incident light. Upon exposure to an interference pattern, a diffusion process is established as the monomer begins to form the polymer network primarily in the bright regions and leads to the mass-transfer of the non-reactive species toward the dark regions by an inverse diffusion process (Fig. 2(c)) [52,53]. Eventually, the liquid crystal concentration exceeds a solubility threshold and nanoscale droplets form surrounded by the polymer matrix. The influence of polymer shrinkage (often $\sim$5–10% in the popular acrylate-based mixtures) has also been

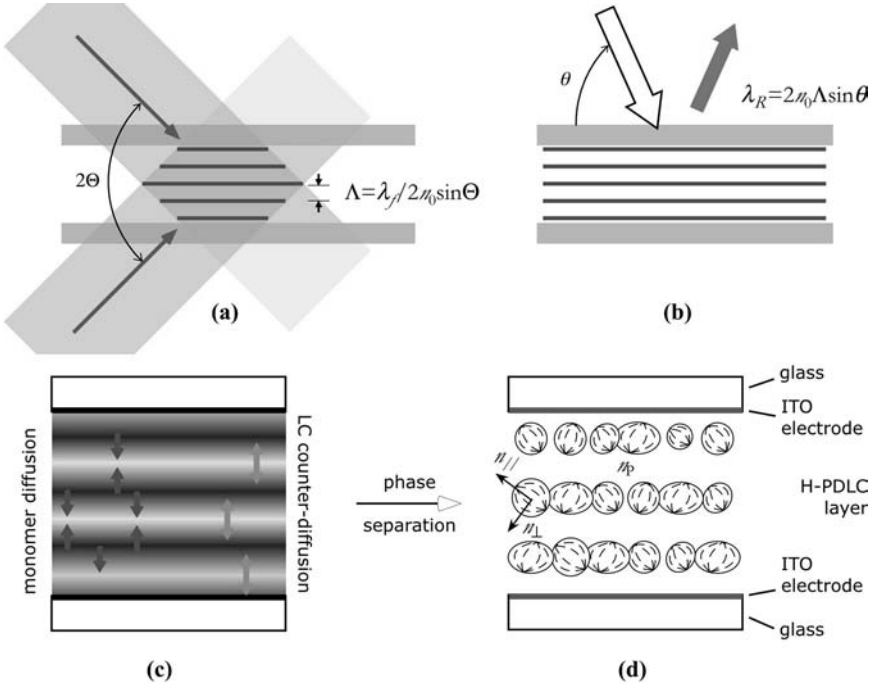

FIGURE 2 Bragg reflection gratings formed in H-PDLCs: (a) two interfering coherent beams created in a spatial variation in the intensity dependant on the angle between the beams and the wavelength; (b) a reflection grating so formed will reflect a narrow range of colors with peak wavelength determined by Bragg's Law; (c) during formation, the spatial intensity variation causes the initially homogeneous mixture of monomer and LC to diffuse and counter-diffuse; (d) eventually, phase separation occurs, and stratified layers of LC droplets are formed within a rigid polymer binder—as with PDLCs, an applied electric field will reduce the index modulation, and the reflection efficiency.

included in diffusion models [54]. The end result is generally a phase-separated film with liquid crystal droplets confined within a polymer binder (Fig. 2(d)). The index modulation between liquid crystal and polymer layers can then be electrically reduced by the application of an electric field, which causes a reorientation of the nematic director configuration within the nanodroplets. It is commonly stated that this occurs when the ordinary index of the liquid crystal ($n_\perp$) matches that of the polymer (n_P). Note however, that the situation is complicated by the fact that a non-negligable amount of liquid crystal almost always remains in the polymer matrix, and a low density polymer network may remain in the liquid crystal region. Therefore, it is more proper to say that the index

modulation is extinguished by the application of an electric field when the ordinary index of the liquid crystal-rich regions equals that of the polymer-rich regions.

In this contribution we focus on the creation of 3D lattices in H-PDLC materials using four beam exposure techniques with dimensions comparable to the wavelength of visible/IR light, which have potential use as photonic crystals. We begin with a review the simple face centered cubic (fcc) lattice [16] and then present data on the diamond-like fcc lattice [55]. The diamond-like lattice has advantages beyond the simple fcc in terms of ease of processing, depth of stopbands, and electro-optic operation in the telecommunication band.

2. MATERIALS

Free radical polymerization at both UV [56–59] and visible wavelengths [3–7,39,60,61] has proven successful to achieve phase separation in H-PDLCs with desirable morphologies, in part because the rapid cross-linking and gellation of the polymer network tends to produce the best phase separation characteristics. For our experiments described in this contribution, the materials were composed of polymer functional oligomers, a nematic liquid crystal (BL038, EM Industries, $T_{NI} = 100^{\circ}C$, $[n_{\parallel}, n_{\perp}] = [1.799, 1.527]$, at 589 nm and $20^{\circ}C$), and a photoinitiator combination sensitized to green wavelengths (Rose Bengal and coinitiator *n*-phenylglycine). The blend contained urethane acrylate tri- and hexa-functional oligomers (procured from UCB-Radcure) combined with n-vinyl-pyrrolidinone (from Sigma-Aldrich). The ratio of monomers, nematic, and photoinitiators was 62:36:2 by weight. An alternative material recipe utilizes dipentaerythritol pentacrylate combined with nematic liquid crystal and a similar photoinitiator recipe [61]. Surfactants are often used in the mixture to reduce the drive voltage [62], and have been known for some time to manipulate the nature of the liquid crystal surface anchoring in confined systems [63].

3. FACE CENTERED CUBIC HOLOGRAMS

For both holograms discussed in this work, we formed the 3D irradiance profile through the interference of four linearly-polarized coherent beams ($\lambda_0 = 532$ nm) from a diode-pumped Nd:YAG laser. Exposure times were usually $\sim$30 sec, followed by several minutes of blanket illumination from a UV lithographic lamp. The holographic parameters (propagation vectors ($\mathbf{k}$) and associated electric field vectors ($\mathbf{A}$)) were determined using standard methods [55,64], and the interference profile was computed by the

following expression:

$$I(\mathbf{r}) \propto R\left\{\sum_{l=1}^{N}\sum_{m=1}^{N}\mathbf{A}_l \cdot \mathbf{A}_m^* e^{[i(k_l-k_m)\cdot \mathrm{r}]}\right\} \tag{1}$$

where the spatial position is defined by a $\mathbf{r} = (\mathrm{X,Y,Z})^T$, the number of coherent beams, and the reciprocal lattice vector $\mathbf{G}_{lm} = \mathbf{k}_l - \mathbf{k}_m$. While we employ Eq. (1) in this case to design fcc lattices, *any* Bravais lattice desired may be formed by the proper choice of the propagation and polarization vectors [12,55,64].

3.1. Simple Face Centered Cubic

The simple fcc lattice was formed using a "symmetric-splitting" technique [16], with four beams of the same intensity (each at $\sim$140 mW/cm^2). The propagation vectors and normalized polarization vectors for this hologram are listed in Table 1, expressed in terms of the lattice constant:

$$D_{\mathrm{simple}} = \sqrt{5}(\lambda_0/n_0)/2. \tag{2}$$

The lattice constant D_{simple} was ideally 384 nm, assuming $n_0 = 1.55$. The following three-dimensional (3D) intensity profile was the anticipated result:

$$I(\mathbf{r}) \propto 4 + \cos(\mathbf{G}_{13}\cdot\mathbf{r}) + \cos(\mathbf{G}_{24}\cdot\mathbf{r}) + \cos(\mathbf{G}_{23}\cdot\mathbf{r}) + \cos(\mathbf{G}_{14}\cdot\mathbf{r}) \tag{3}$$

Several calculated iso-intensity surfaces for this photonic crystal are shown in Figure 3, of which part (b) and (c) correspond best to the anticipated polymer and liquid crystal droplet morphology, respectively. Figure 3(d) corresponds to the substrate orientation relative to the coordinate system. In Figure 3(e), the exposure configuration is disclosed, where two beams are incident from above and two from below, coupled into the H-PDLC film using 90° prisms in order to attain the required propagation angles. As reported previously [16], a completely reversible 2% wavelength shift of the [$\pm$1 1 1] stop band was observed upon the application of an electric field. We have included a summary of the simple fcc lattice here for completeness and for comparison with the diamond-like fcc lattice, which is the subject of this paper.

3.2. Diamond-like Face Centered Cubic

Our recent investigations with the diamond-like fcc hologram with an asymmetric basis (based on the earlier studies of Campbell and coworkers [55] who investigated this lattice in the negative-tone epoxy resist SU-8) highlight several advantages. First, no coupling prisms are required to form

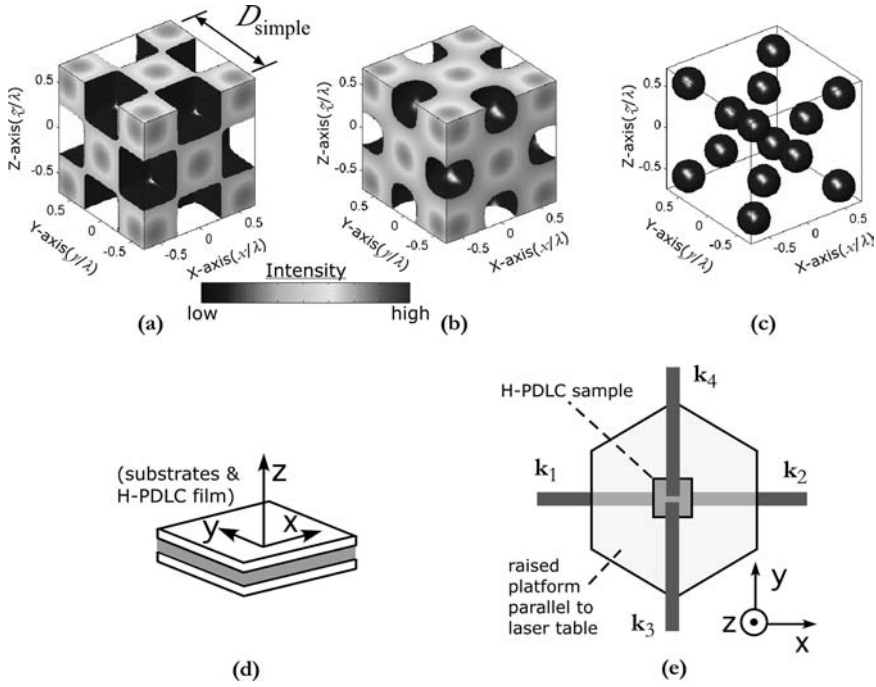

FIGURE 3 The simple fcc lattice: (a) calculated irradiance profile—the iso-intensity surface value was chosen to give cubic "atoms" at each lattice site; (b) a more realistic iso-intensity choice leads to the profile corresponding the expected polymer morphology and (c) LC spatial distribution when the LC loading is around 35%; (d) substrate orientation relative to coordinate system; (e) view of fabrication platform from "above".

this lattice, simplifying the setup and resulting in a substantially larger lattice constant; unlike the previous lattice (simple fcc) with a $D_{\text{simple}} \sim 1.1\lambda_0$, this configuration leads to $D_{\text{diamond-like}} \sim 2.6\lambda_0$, and allows visible and UV lasers to generate photonic crystals with stopbands at the IR telecommunications bands from $\sim 900\,\text{nm} \rightarrow 1570\,\text{nm}$. Second, the lattice orientation is rotated such that light normally incident on the substrates propagates along the [1 1 1] direction of the fcc lattice. Third, there are potentially wider and deeper stopbands in this lattice for the same given materials, as it is akin to the diamond crystal structure.

The calculated iso-intensity surface of this hologram are illustrated in Figure 4(a) such that the [1 0 0], [0 1 0], and [0 0 1] lattice planes are parallel to the X, Y, and Z-axes. The nature of the fcc lattice can be clearly seen. However, our actual holographic setup (using an "umberellalike"

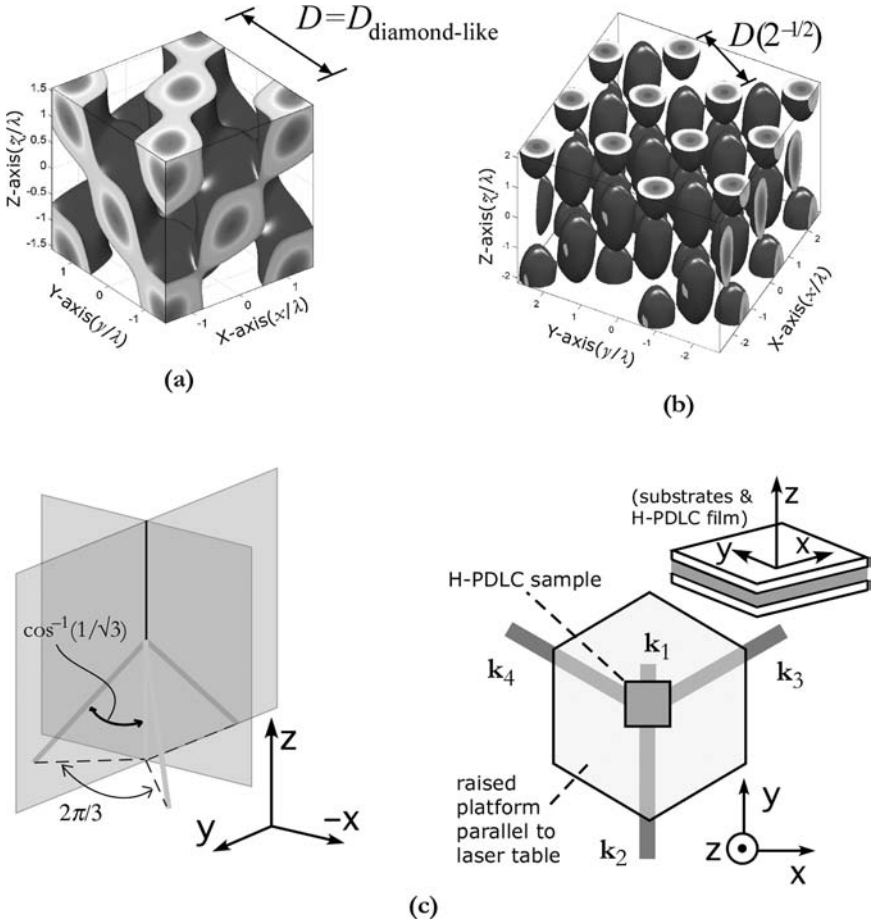

FIGURE 4 The diamond-like fcc lattice: (a) calculated irradiance profile with [0 0 1] lattice plane parallel to the XY-plane, highlighting fcc nature of irradiance profile; (b) calculated irradiance profile with [1 1 1] lattice plane parallel to the XY-plane, which results from the actual holographic setup—notice the hexagonal arrangement of "atoms" in the top layer; (c) the "umbrellalike" four-beam hololithography setup illustrated from a perspective view; (d) overhead view illustrated from above, highlighting sample orientation with respect to the holography.

technique) led to a different lattice orientation, such that the [1 1 1]-planes was parallel to the XY plane, as calculated in Figure 4(b). Two views of the beam setup are shown in Figure 4(c), along with the relative orientation of the substrates. Unlike the previous hologram, the beams did not have equal

intensities (the beam along the Z axis was $\sim 375\,\mathrm{mW/cm^2}$, and the others were each set to $\sim 75\,\mathrm{mW/cm^2}$). The propagation and electric-field vectors are listed in Table 2, while the new lattice constant and normalized irradiance profile are shown below:

$$D_{\text{diamond-like}} = 3\sqrt{3}(\lambda_0/n_0)/2 \tag{4}$$

$$I(\mathbf{r}) \propto 8 \; + \; 3.4\cos(\mathbf{G}_{12}\cdot\mathbf{r}) + 4.45\cos(\mathbf{G}_{13}\cdot\mathbf{r}) - 3.56\cos(\mathbf{G}_{14}\cdot\mathbf{r}) + 1.39\cos(\mathbf{G}_{23}\cdot\mathbf{r}) - 1.08\cos(\mathbf{G}_{24}\cdot\mathbf{r}) - 1.67\cos(\mathbf{G}_{34}\cdot\mathbf{r}) \tag{5}$$

The constant $D_{\text{diamond-like}}$ was therefore ideally 892 nm, and the fabricated films should reflect normally-incident light at 1596 nm from the [1 1 1] lattice direction. A series of lower notches in the transmission is expected from the other lattice planes, most notably a notch at ~ 532 nm from the $[1\,\bar{1}\,1]/[\bar{1}\,1\,1]/[\bar{1}\,\bar{1}\,1]$–planes, and at ~ 800 nm from the $[1\,0\,0]/[0\,1\,0]/[0\,0\,1]$–planes, when normally incident to the substrate.

The measured transmittance is shown in Figure 5 for on- and off-axis visible light. Note the relatively broad notch centered at 560 nm when viewed on-axis arising from the slightly misaligned $[1\,\bar{1}\,1]/[\bar{1}\,1\,1]/[\bar{1}\,\bar{1}\,1]$ lattice planes (all Bragg-matched for the same wavelength for light normally incident). When the sample is tilted off axis by $\sim 5^\circ$ toward one of these planes, this single notch splits into three, as shown in Figure 5. This occurs since the tilt

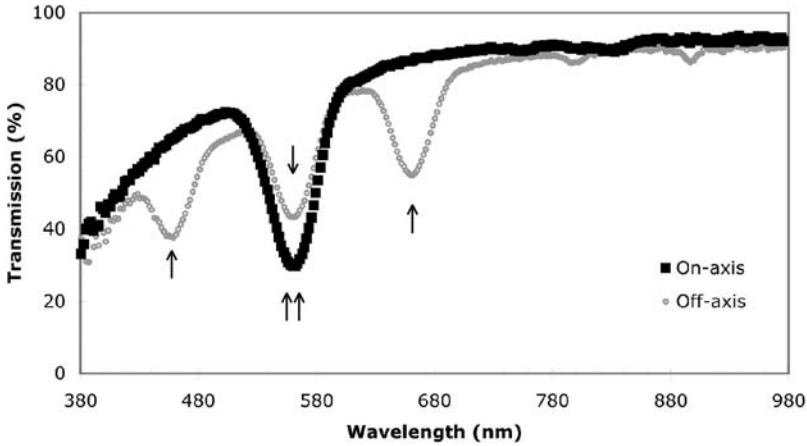

FIGURE 5 Transmission spectra of the diamond-like fcc lattice over visible wavelengths for on-axis and off-axis (by about 5°) light. The peak indicated by the double arrows is caused by the three Bragg-matched $[1\,\bar{1}\,1]/[\bar{1}\,1\,1]/[\bar{1}\,\bar{1}\,1]$ lattice planes. The peaks indicated by the single arrows arise as the incident meets each of the three previously mentioned lattice planes at different angles leading to different Bragg conditions.

causes light to be incident on two of the lattice planes at different angles and leads to different Bragg-matched wavelengths for each.

The on-axis transmission was recorded as an electric field was applied; the electro-optic response of the notch at 560 nm is plotted in Figure 6(a). As expected, there was minimal wavelength-shift; but most notably, no substantial field threshold was manifest, and the electro-optic switching begins with almost any field. Highly different from other H-PDLC gratings, one explanation for this arises from the expected shape of LC droplets, which has been calculated and is shown in Figure 6(b). In cross-section, it is apparent that these domains are roughly ellipsoidal, with a major axis parallel to the [1 1 1] lattice direction and the direction of the applied electric field. The switching analysis reported by Wu and coworkers for conventional PDLCs does not adequately describe this circumstance, even

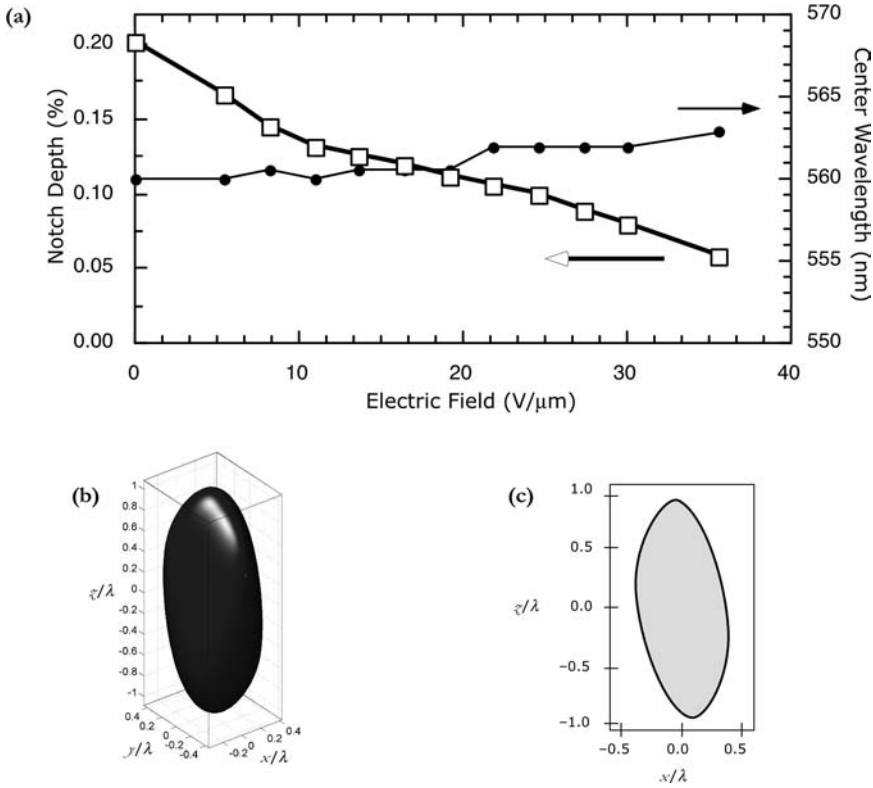

FIGURE 6 (a) Electro-optic switching of the diamond-like fcc lattice with on-axis light. (b) Anticipated LC droplet volume, calculated from the irradiance profile; (c) Cross-section of the same, showing the skewed ellipsoidal nature of the droplet.

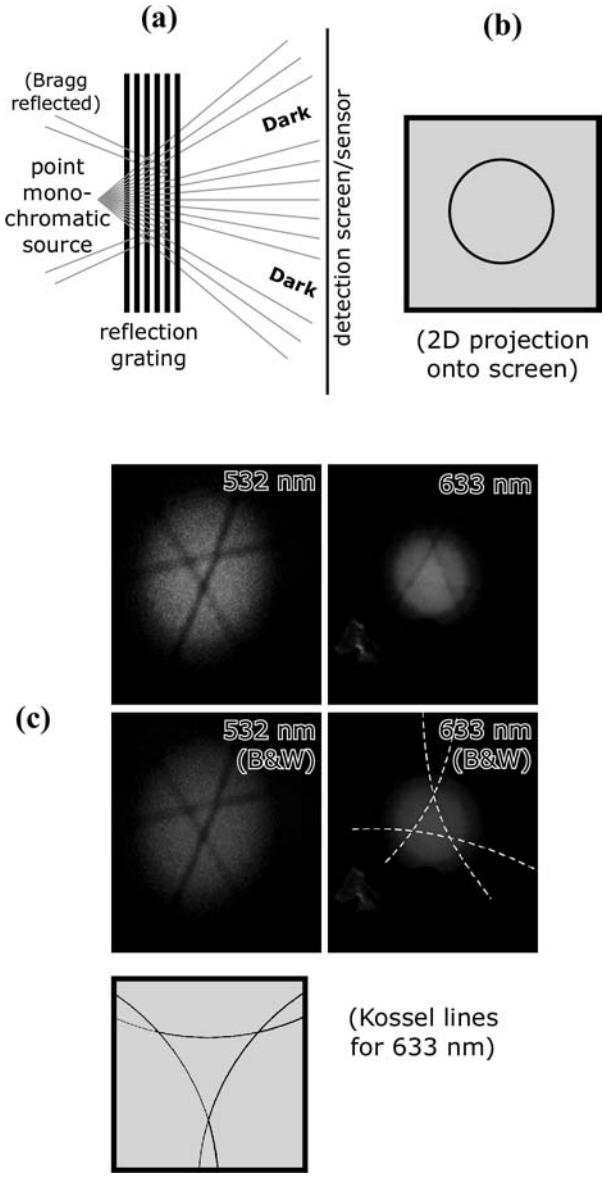

FIGURE 7 The principle of Kossel diffraction: (a) a simple reflection grating Bragg reflects for only a narrow range of angles while all other angles pass through unscattered; (b) projected onto a screen, a two-dimensional image of dark curves within a bright field results. In this simple case, only a circle appears. (c) The Kossel patterns of the diamond-like fcc—measured with both a red and green wavelength.

if the LC configuration were known, since the applied field is parallel to the major axis of the ellipsoid. As we strongly suspect planar anchoring, the field would likely lead to elastic deformation, and more precise numerical methods must be utilized.

The most thorough way to optically examine the 3D nature of a crystal (photonic *or* atomic) is to examine its Kossel ring Bragg diffraction pattern [16,55]. It requires the use of a point source of monochromatic light (such as can be generated from a laser with an appropriate lens or fiber-optic arrangement) positioned adjacent to the crystal such that a broad range of angles is simultaneously incident upon the sample. The output is then examined as the intensity for a given angle, a 2D image. This is illustrated in Figure 7(a) for a single reflection grating probed with wavelength slightly lower than the Bragg-matched wavelength, as an example. In this way, there are angles for which the transmission is suppressed. For the case of the single reflection grating in our example, a dark circle will appear. For more complex lattices, various textures in the two-dimensional output are seen, and can be directly related to the fcc lattice structure.

The Kossel diffraction patterns (probed using light at 532 nm) of the diamond-like fcc lattices formed in H-PDLCs are shown in Figure 7(b). Note that three intersecting hyperbolic lines arise from the $[1\,\bar{1}\,1]$/$[\bar{1}\,1\,1]$/$[\bar{1}\,\bar{1}\,1]$–planes. While these characterizations could be pursued further at wider angles and various wavelengths, they clearly show the 3D fcc nature of our fabricated lattice.

4. DISCUSSION AND CONCLUSIONS

Several groups [14–17] suggest H-PDLC materials as a novel approach to tuning functionality in the PhC context, due their comparatively fast/simple fabrication and the great design flexibility in lattice parameters (e.g. type, crystal basis, and size). Certain limitations are nonetheless apparent: a relatively small refractive index contrast is inherent to the materials, incoherent scattering is caused by droplet and director irregularities, and anisotropic shrinkage of the acrylate systems can cause some lattice distortion. Further research efforts are directed toward the improvement of these issues.

In this paper we have briefly reviewed the field of H-PDLC devices and described the successful fabrication of two face centered cubic lattices by holographic means using a switchable LC/polymer material, and characterized their electro-optical properties and 3D lattice structure. The diamond-like fcc configuration may have more utility in telecommunications applications (than the simple fcc lattice) since it operates in the near

infrared spectral region, has the potential for a deeper stopbands, and is easier to fabricate since no coupling prisms are needed during exposure.

REFERENCES

[1] Drzaic, P. S. 1995. *Liquid crystal dispersions*, World Scientific: Singapore.
[2] Crawford, G. P. (2003). *Optics and Photonics News*, *14*, 54.
[3] Bunning, T. J., Natarajan, L. V., Tondiglia, V. P. & Sutherland, R. L. (2000). *Annu. Rev. Mater. Sci.*, *30*, 83.
[4] Sutherland, R. L., Natarajan, L. V., Tondiglia, V. P., & Bunning, T. J. (2000). In: *Handbook of Advanced Electronic and Photonic Materials and Devices*, Nalwa, H. S. (Eds.), Academic Press: San Diego.
[5] Tanaka, K., Kato, K., Date, M., & Sakai, S. (1995). *SID Digest Technol. Pap.*, *XXVI*, 267.
[6] Crawford, G. P., Fiske, T. G., & Silverstein, L. D. (1996). *SID Digest Technol. Pap.*, *XXVII*, 99.
[7] Bunning, T. J., Natarajan, L. V., Sutherland, R. L., & Tondiglia, V. P. (2000). *SID Digest Technol. Pap.*, *XXXI*, 121.
[8] Domash, L. H., Chen, Y.-M., Gozewski, C., Haugsjaa, P., & Oren, M. (1997). *Proc. SPIE.*, *3010*, 214.
[9] Yeralan, S., Gunther, J., Ritums, D., Cid, R., & Popovich, M. (2002). *Opt. Eng.*, *41*, 1774.
[10] Ogiwara, A., Kuratomi, Y., Karasawa, T., Takimoto, A., & Mizuguchi, S. (1999). *SID Digest Technol. Pap.*, *XXX*, 90.
[11] Domash, L. H., Chen, Y.-M., Gomatam, B. N., Gozewski, C. M., Sutherland, R. L., Natarajan, L. V, Tondiglia, V. P., Bunning, T. J., & Adams, W. W. (1996). *Proc. SPIE*, *188*, 2689.
[12] Escuti, M. J. & Crawford, G. P. (2002). *SID Digest Technol. Pap*. *XXXIII*, 90.
[13] Escuti, M. J. & Crawford, G. P. (2002). *Asia Display*, *8*, LCST-08.
[14] Tondiglia, V. P., Natarajan, L. V., Sutherland, R. L., Tomlin, D., & Bunning, T. J. (2002). *Adv. Mater.*, *14*, 187.
[15] Sutherland, R. L., Tongdiglia, V. P., Natarajan, L. V., & Chandra, S. (2002). *Opt. Ex.*, *10*, 1074.
[16] Escuti, M. J., Qi, J., & Crawford, G. P. (2003). *Opt. Lett.*, *28*, 522.
[17] Escuti, M. J., Qi, J., & Crawford, G. P. (2003). *Appl. Phys. Lett.*, *83*, 1331.
[18] Jakubiak, R., Bunning, T. J., Vaia, R. A., Natarajan, L. V., & Tondiglia, V. P. (2003). *Adv. Mat.*, *15*, 241.
[19] Sutherland, R. L., Natarajan, L. V., Tongdiglia, V. P., & Crane, R. L. (1997). U.S. Patent 5, 698, 343.
[20] Cairns, D. R., Bowley, C. C., Danworaphong, S., Fontecchio, A. K., Crawford, G. P., Li, L., & Faris, S. M. (2000). *Appl. Phys. Lett.*, *77*, 2677.
[21] Fiske, T. G., Silverstein, L. D., Colegrove, J., & Yuan, H. (2000). *SID Digest Technol. Pap*, *XXXI*, 1134.
[22] Domash, L. H., Crawford, G. P., Ashmead, A. C., Smith, R. T., Popovich, M. M., & Storey, J. (2000). *Proc. SPIE*, 4107.
[23] Simoni, F., Cipparrone, G., Mazzulla, A., & Pagliusi, P. (1999). *Chem. Phys.*, *245*, 429.
[24] Fuh, A. Y. G., Liao, C. C., & Tsai, C. Y. (2001). *Opt. Lett.*, *26*, 447.
[25] Fontecchio, A. K., Bowley, C. C., & Crawford, G. P. (1999). *Proc. SPIE*, *3080*, 36.
[26] Qi, J., Xianyu, H., Liang, J., & Crawford, G. P. (2003). *IEEE Phot. Lett.*, *15*, 685.
[27] Popovich, M. & Sagan, S. (2000). *SID Digest Technol. Pap.*, *XXXI*, 1060.

[28] Jazbinsek, M., Drevensek-Olenik, I., Zgonik, M., Fontecchio, A. K., & Crawford, G. P. (2001). *J. Appl. Phys.*, *90*, 3831.
[29] Sutherland, R. L. (2002). *J. Op. Soc. Am.*, *19*, 2995.
[30] Sutherland, R. L., Natarajan, L. V., Bunning, T. J., Tondiglia, V. P., Brandelik, D., Shepherd, C. K., Chandra, S., & Siwecki, S. (2002). *J. Op. soc. Am. B*, *19*, 3004.
[31] Holmes, M. E. & Malcuit, M. S. (2002). *Phys. Rev. E*, *65*, 066603–1.
[32] Vardanyan, K., Qi, J., Eakin, J. N., DeSarkar, M., & Crawford, G. P. (2002). *Appl. Phys. Lett.*, *81*, 4736.
[33] Vilfan, M., Zalar, B., Fontecchio, A. K., Vilfan, M., Escuti, M. J., Crawford, G. P., & Zumer, S. (2002). *Phys. Rev. E*, *66*, 021710.
[34] Vaia, R. A., Tomlin, D. W., Schulte, M. D., & Bunning, T. J. (2001). *Polymer*, *42*, 1055.
[35] Bharadwaj, R. K., Bunning, T. J., & Farmer, B. L. (2000). *Liq. Cryst.*, *27*, 591.
[36] Kyu, T., Nwabuma, D., & Chiu, H. W. (2001). *Phys. Rev. E*, *63*, 061802.
[37] Kato, K., Hisaki, T., & Date, M. (1999). *Jpn. J. Appl. Phys.*, *38*, 1466.
[38] Date, M., Takeuch, Y., & Kato, K. (1999). *J. Phys. D*, *32*, 3164.
[39] Bowley, C. C., Crawford, G. P. & Yuan, H. (1999). *Appl. Phys. Lett.*, *74*, 3096.
[40] Boiko, Y., Eakin, J., Vedrine, J., & Crawford, G. P. (2002). *Opt. Lett.*, *27*, 1717.
[41] Date, M., Takeuch, Y., & Kato, K. (1999). *J. Phys. D*, *32*, 3164.
[42] Bunning, T. J., Kirkpatrick, S. M., Natarajan, L. V., Tondiglia, V. P., & Tomlin, D. W. (2000). *Chem. Mater.*, *12*, 2842.
[43] Bowley, C. C., Kossyrev, P. A., Crawford, G. P., & Faris, S. (2001). *Appl. Phys. Lett.*, *79*, 9.
[44] Cipparrone, G., Mazzulla, A., & Russo, G. (2001). *Appl. Phys. Lett.*, *78*, 1186.
[45] Qi, J., Sousa, M. E., Fontecchio, A. K, & Crawford, G. P. (2003). *Appl. Phys. Lett.*, *82*, 1652.
[46] Bowley, C. C., Fontecchio, A. K., Crawford, G. P., Lin, J.-J., Li, L., & Faris, S. (2000). *Appl. Phys. Lett.*, *76*, 523.
[47] Escuti, M. J. P., Kossyrev, P. A., Crawford, G. P., Fiske, T. G., Colgrove, J., & Silverstein, L. D. (2000). *Appl. Phys. Lett.*, *77*, 4262.
[48] Fuh, A. Y. G., Lee, C. R., & Mo, T. S. (2002). *J. Opt. Soc. Am. B*, *19*, 2590.
[49] Fuh, A. Y. G., Lee, C. R., & Ho, Y. S. (2001). *Jpn. J. Appl. Phys.*, *40*, 6868.
[50] Fuh, A. Y. G., Lee, C. R., & Mo, T. S. (2002). *Appl. Optics*, *41*, 4585.
[51] Xianyu, H., Qi, J., Cohn, R. F., & Crawford, G. P. (2003). *Opt. Lett.*, *28*, 792.
[52] Caputo, R., Sukhov, A. V., & Tabiryan, N. V. (2002). *Mol. Cryst. Liq. Cryst.*, *372*, 263.
[53] Bowley, C. C. & Crawford, G. P. (2000). *Appl. Phys. Lett.*, *76*, 2235.
[54] Qi, J., DeSarker, M., Warren, G. T., & Crawford, G. P. (2002). *J. Appl. Phys.*, *91*, 4795.
[55] Campbell, M., Sharp, D. N., Harrison, M. T., Denning, R. G., & Turberfield. (2000). *Nature*, *404*, 53.
[56] Duca, D., Sukhov, A. V., & Umeton. (1999). *Liq. Cryst.*, *26*, 931.
[57] DeSarkar, M., Qi, J., & Crawford, G. P. (2002). *Polymer*, *43*, 7335.
[58] DeSarkar, M., Gill, N. L., Whitehead, J. B., & Crawford, G. P. (2003). *Macromol.*, *36*, 630.
[59] Natarajan, L. V., Shepherd, C. K., Brandelik, D. M., Sutherland, R. L., Chandra, S., Tondiglia, V. P., Tomlin, D., & Bunning, T. J. (2003). *Chem. Mater.*, *15*, 2477.
[60] Date, M., Takeuchi, Y., Tanaka, K., & Kato, S. (1998). *J. Soc. Inf. Display*, *6*, 37.
[61] Sutherland, R. L., Natarajan, L. V., Tondiglia, V. P., & Bunning, T. J. (1993). *Chem. Mater.*, *5*, 1533.
[62] Yuan, H., Hu, G., Fiske, T. G., Gunther, J. E., Silverstein, L. D., Bowley, C. C., Crawford, G. P., Chien, L. C., & Kelly, J. R. (1998). *Proc. Asia Display*, *98*, 1171.
[63] Crawford, G. P., Ondris-Crawford, R. J., Doane, J. W., & Zumer, S. (1993), *Phys. Rev. Lett.*, *70*, 1838; *Phys. Rev. E*, *35*, 3674 (1996).
[64] Cai, L. Z., Yang, X. L., & Wang, Y. R. (2002). *J. Opt. Soc. Am. A*, *19*, 2238.